



RESEARCH ARTICLE

10.1002/2015GB005183

Key Points:

- Oxygen in North Atlantic STUW has decreased ~25 micromoles/kg since 1980
- Changes in STUW oxygen are driven by climate forcing in the North Atlantic
- Oceanographic time series stations capture oxygen variability in STUW

Supporting Information:

- Figure S1

Correspondence to:

E. Montes,
emontesh@mail.usf.edu

Citation:

Montes, E., F. E. Muller-Karger, A. Cianca, M. W. Lomas, L. Lorenzoni, and S. Habtes (2016), Decadal variability in the oxygen inventory of North Atlantic subtropical underwater captured by sustained, long-term oceanographic time series observations, *Global Biogeochem. Cycles*, 30, 460–478, doi:10.1002/2015GB005183.

Received 13 MAY 2015

Accepted 13 FEB 2016

Accepted article online 17 FEB 2016

Published online 12 MAR 2016

Corrected 28 MAR 2016

This article was corrected on 28 MAR 2016. See the end of the full text for details.

Decadal variability in the oxygen inventory of North Atlantic subtropical underwater captured by sustained, long-term oceanographic time series observations

Enrique Montes¹, Frank E. Muller-Karger¹, Andrés Cianca², Michael W. Lomas³, Laura Lorenzoni¹, and Sennai Habtes⁴

¹College of Marine Science, University of South Florida, St. Petersburg, Florida, USA, ²Instituto Canario de Ciencias Marinas, Gobierno de Canarias, Telde, Spain, ³Bigelow Laboratory for Ocean Sciences, Boothbay Harbor, Maine, USA, ⁴Center for Marine and Environmental Studies, University of the Virgin Islands, St. Thomas, Virgin Islands, USA

Abstract Historical observations of potential temperature (θ), salinity (S), and dissolved oxygen concentrations (O_2) in the tropical and subtropical North Atlantic (0–500 m; 0–40°N, 10–90°W) were examined to understand decadal-scale changes in O_2 in subtropical underwater (STUW). STUW is observed at four of the longest, sustained ocean biogeochemical and ecological time series stations, namely, the Carbon Retention In A Colored Ocean (CARIACO) Ocean Time Series Program (10.5°N, 64.7°W), the Bermuda Atlantic Time-series Study (BATS; 31.7°N, 64.2°W), Hydrostation “S” (32.1°N, 64.4°W), and the European Station for Time-series in the Ocean, Canary Islands (ESTOC; 29.2°N, 15.5°W). Observations over similar time periods at CARIACO (1996–2013), BATS (1988–2011), and Hydrostation S (1980–2013) show that STUW O_2 has decreased approximately 0.71, 0.28, and 0.37 $\mu\text{mol kg}^{-1} \text{yr}^{-1}$, respectively. No apparent change in STUW O_2 was observed at ESTOC over the course of the time series (1994–2013). Ship observation data for the tropical and subtropical North Atlantic archived at NOAA National Oceanographic Data Center show that between 1980 and 2013, STUW O_2 (upper ~300 m) declined 0.58 $\mu\text{mol kg}^{-1} \text{yr}^{-1}$ in the southeastern Caribbean Sea (10–15°N, 60–70°W) and 0.68 $\mu\text{mol kg}^{-1} \text{yr}^{-1}$ in the western subtropical North Atlantic (30–35°N, 60–65°W). A declining O_2 trend was not observed in the eastern subtropical North Atlantic (25–30°N, 15–20°W) over the same period. Most of the observed O_2 loss seems to result from shifts in ventilation associated with decreased wind-driven mixing and a slowing down of STUW formation rates, rather than changes in diffusive air-sea O_2 gas exchange or changes in the biological oceanography of the North Atlantic. Variability of STUW O_2 showed a significant relationship with the wintertime (January–March) Atlantic Multidecadal Oscillation index (AMO, $R^2 = 0.32$). During negative wintertime AMO years trade winds are typically stronger between 10°N and 30°N. These conditions stimulate the formation and ventilation of STUW. The decreasing trend in STUW O_2 in the three decades spanning 1980 through 2013 reflects the shift from a strongly negative wintertime AMO between the mid-1980s and mid-1990s to a positive wintertime AMO observed between the mid-1990s and 2013. These changes in STUW O_2 were captured by the CARIACO, BATS, and Hydrostation S time series stations. Sustained positive AMO conditions could lead to further deoxygenation in tropical and subtropical North Atlantic upper waters.

1. Introduction

The concentration of dissolved oxygen (O_2) in a water parcel at the ocean surface is a balance determined by air-sea gas exchange, vertical and horizontal diffusion and mixing, and by biological productivity and respiration processes [Emerson *et al.*, 2004; Deutsch *et al.*, 2005]. Vertical profiles of dissolved O_2 collected in the ocean interior over the last ~50 years suggest that thermocline O_2 is decreasing globally at rates between 0.3 and 0.7 $\mu\text{mol kg}^{-1} \text{yr}^{-1}$ [García *et al.*, 1998; Emerson *et al.*, 2001, 2004; Joos *et al.*, 2003; Deutsch *et al.*, 2005; Johnson and Gruber, 2007; Stendardo and Gruber, 2012; Stramma *et al.*, 2008, 2012; Tanhua and Keeling, 2012; Emerson and Bushinsky, 2014, and others]. There are still large gaps in our understanding of how O_2 varies within middle- to low-latitude epipelagic water masses. In this study, we examine the mechanisms that control the O_2 inventory of North Atlantic subtropical underwater (STUW), a shallow (0 to ~300 m), high-salinity (>36) water mass distributed across tropical and subtropical latitudes [Wust, 1964; O'Connor *et al.*, 2005]. STUW is observed at four of the longest sustained ocean biogeochemical and ecological time series stations in the North Atlantic, namely, the CARIACO Ocean Time Series (10.5°N, 64.7°W), the Bermuda Atlantic Time-series Study (BATS; 31.7°N, 64.2°W), Hydrostation “S” (32.1°N, 64.4°W), and the

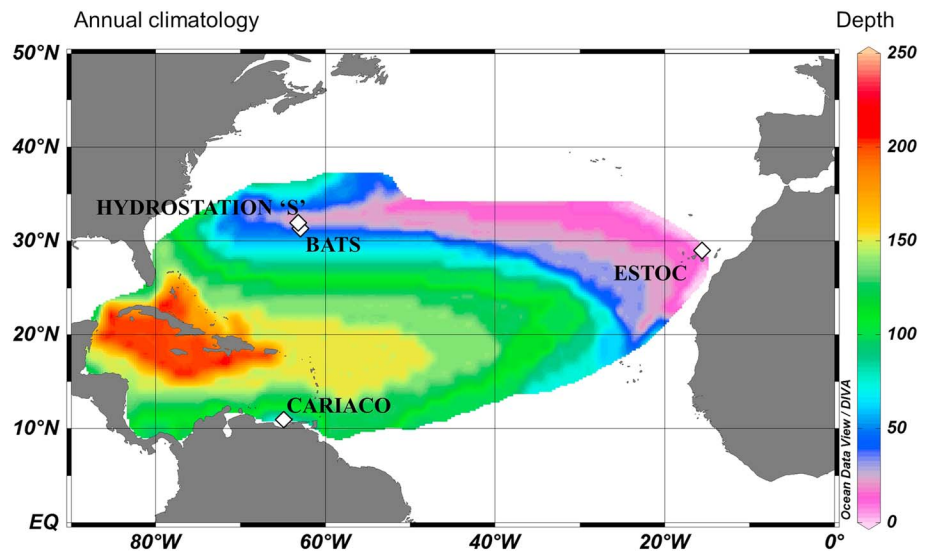


Figure 1. Climatological annual average depth of the core of the North Atlantic STUW. The locations of the ESTOC, BATS, Hydrostation "S", and CARIACO time series stations are shown with white diamonds.

European Station for Time-series in the Ocean, Canary Islands (ESTOC; 29.2°N, 15.5°W; Figure 1). We seek to determine whether these stations capture regional O₂ trends observed within STUW in historical hydrographic data. We also examine the causes of the decadal-scale variability observed in STUW O₂ since 1950.

Data collected over the last five decades show that oxygen minimum zones in the Atlantic and the Pacific Oceans have expanded, leading to habitat reduction for tropical pelagic fishes of up to 15% [Prince and Goodyear, 2006; Stramma *et al.*, 2010, 2012; Prince *et al.*, 2010; Ekau *et al.*, 2010]. Further ecosystem compression from reduction of O₂ in eastern boundary current systems and in other pelagic ecosystem is expected as a result of increasing water column stratification, shifts in basin-wide circulation patterns, declines in thermocline ventilation rates, and rising average global temperatures [Keeling and García, 2002; Bopp *et al.*, 2013; Frölicher *et al.*, 2009; Meehl *et al.*, 2007; Keeling *et al.*, 2010].

To adequately evaluate decadal-scale changes in oceanic O₂ pools, it is necessary to collect relatively good spatial coverage of O₂ profiles across ocean basins over several decades. Although the spatial density of O₂ observations obtained by hydrographic cruises and autonomous platforms such as profiling floats, moorings, and gliders has become more abundant since the 1950s, these measurements are not consistently accompanied by the biogeochemical observations (e.g., inorganic nutrients, dissolved organic matter, settling particulate organic matter, and primary productivity) needed for a comprehensive understanding of O₂ cycling in the ocean. Biogeochemical and ecological ocean time series stations sustained over several decades are the only platforms that have provided high-quality O₂ and other chemical, biological, and physical measurements needed for studying oceanic O₂ dynamics [Whitney *et al.*, 2007; Church *et al.*, 2013]. These observations, however, have limited spatial coverage because they are conducted at a fixed location. To put these O₂ measurements into a larger spatial context, we can use high-quality hydrographic measurements gathered in the global ocean since about 1950.

In this study we hypothesize that long-term changes are taking place in the O₂ of subtropical underwater (STUW) of the North Atlantic Ocean. Subtropical underwater forms in the surface eastern subtropical North Atlantic and spreads westward throughout the North Atlantic basin along the 26 σ_θ isopycnal (Figure 1). STUW plays an important role in the ocean-atmosphere heat exchange and hydrological cycle [Gu and Philander, 1997; Curry *et al.*, 2003; Schott *et al.*, 2004; O'Connor *et al.*, 2005]. This is also the water mass observed in the upwelling along the southern Caribbean Sea and around the periphery of the Gulf of Mexico [e.g., Rueda-Roa and Muller-Karger, 2013; Muller-Karger *et al.*, 1991].

STUW forms as a high-salinity water in the central subtropical North Atlantic gyre (15–30°N, 25–55°W) and is later subducted into the upper pycnocline [Doney *et al.*, 1998; Qu *et al.*, 2013; Shcherbina *et al.*, 2015]. Subduction rates are variable, but they are generally higher at the end of winter and early spring, when

Table 1. STUW Properties as Defined by *O'Connor et al.* [2005] and as Used in This Study^a

	<i>O'Connor et al.</i> [2005]		This Study		Observed Mean
	Mean	Range	Mean	Range	
S	36.73	36.72–37.10	36.80	36.50–37.10	36.84 ± 0.22
θ (°C)	20.4	20.4–22.2	21.8	20.5–23.0	21.6 ± 0.7
σ_θ (kg m ⁻³)	26.0	25.6–26.3	25.7	25.1–26.2	25.72 ± 0.25

^aThe “Mean” is calculated from “Range” values, and the “Observed Mean” is calculated using all the data used in this study.

density of the water at the surface is highest. This process is unevenly distributed in space. The properties of this intermediate water mass are defined by its last contact with the atmosphere in the core of the high surface salinity region. Because of the relatively short residence time (<10 years) and high subduction rates of STUW, this water mass is a good index for observing potential changes in global climate [*Shcherbina et al.*, 2015].

Once subducted, STUW spreads laterally in the subtropical gyre. It reaches the North Atlantic western boundary current within 2 years, crossing the Caribbean Sea by the end of 5 years [*Qu et al.*, 2013]. From there, most (~70%) of the subducted STUW turns northward as part of the Florida Current and the Gulf Stream and reaches the subpolar region in about 10 years. When it reaches the North Atlantic Deep Water formation region, it is again subducted and becomes part of the Atlantic Meridional Overturning Circulation [*Qu et al.*, 2013].

We examined recent multidecadal trends in STUW O₂ concentration using O₂ observations collected since 1955 at Hydrostation “S”, and the early to mid-1990s at the CARIACO, BATS, and ESTOC time series stations, as well as discrete O₂ records collected by ships across the tropical and subtropical North Atlantic since the 1950. We used the results to better understand the mechanisms that drive the variability observed in North Atlantic STUW O₂.

2. Methods

2.1. Multiplatform Data Sets

Multiplatform (i.e., cruise discrete samples and CTD casts, autonomous profiling floats and drifters, gliders, and moored buoys) epipelagic and mesopelagic (0–500 m) observations of potential temperature (θ) and salinity (S) collected in the North Atlantic (0–40°N, 10–90°W) between 1900 and 2013 (103 years) were obtained from the National Oceanographic Data Center (World Ocean Database WOD13; National Oceanographic Data Center (NODC)-NOAA). Multiplatform θ and S observations were used for studying the spatial distribution of STUW. Shipboard discrete dissolved O₂ measurements (bottle data only) from the same region collected between 1911 and 2013 were also obtained from WOD13. The data included observations from the CARIACO and BATS programs (including Hydrostation “S” data). ESTOC data were obtained from the Plataforma Oceánica de Canarias. Locations of these time series stations are shown in Figure 1.

The 1900–2013 WOD13 data set included 430,292 vertical profiles of θ and S (49% shipboard, 19% profiling floats, 14% gliders, 12% undulating oceanographic recorders, 6% moored buoys, and 1% bucket samples) and 98,522 bottle O₂ casts.

To study the average regional and vertical distributions of North Atlantic STUW and of STUW O₂ concentrations, we used the climatological objectively interpolated mean fields (1° × 1°) from the NODC’s World Ocean Atlas (WOA09). The spatial domain of STUW was thus defined using the WOA09 climatology. Contour maps of these distributions were constructed using Ocean Data View [*Schlitzer*, 2012]. WOD13 and WOA09 data sets were further processed with MATLAB R2014b (Mathworks®).

2.2. STUW O₂ Analyses

The North Atlantic STUW properties were defined according to *Wust* [1964] and *O'Connor et al.* [2005] and based on the range of variability of S and θ in waters with a potential density (σ_θ) between 25.6 and 26.3 kg m⁻³ (upper and lower STUW isopycnals) as measured at CARIACO, BATS, Hydrostation “S”, and ESTOC (Table 1 and Figure 2). We modified the STUW definition of *O'Connor et al.* [2005] (Table 1) to include O₂ values measured in STUW within surface layers, which can exhibit slightly warmer θ and lower S a result of

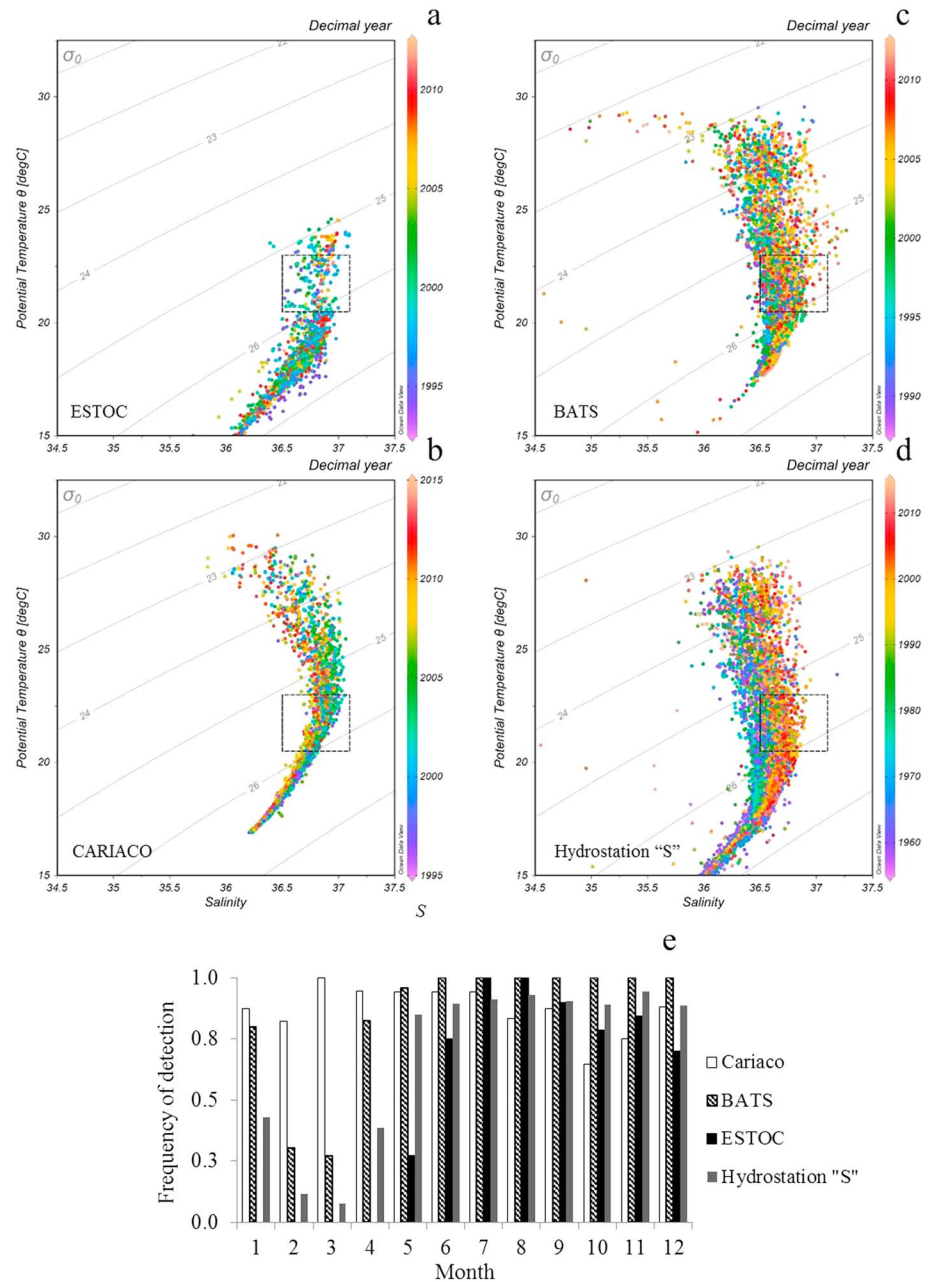


Figure 2. Potential temperature versus salinity ($\theta - S$) at (a) ESTOC, (b) CARIACO, (c) BATS, and (d) Hydrostation "S". The black inset box in each plot indicates $\theta - S$ values that fall within the limits of STUW properties. The color scale bar indicates the year of collection of $\theta - S$ data at monthly resolution. (e) Also shown is the frequency of detection of STUW at each time series site.

higher exposure to solar radiation and precipitation. Climatological (WOA09 data) distributions of O_2 were examined by excluding all measurements in waters with properties outside those of STUW.

To understand how STUW O_2 has changed over time, WOD13 O_2 observations in waters with θ and S outside the limits of STUW (Table 1) were excluded from the analyses. WOD13 observations collected outside the climatological domain of North Atlantic STUW as defined by the climatological (WOA09) spatial distribution of STUW (see Figure 1) were also excluded. STUW O_2 observations were then binned horizontally at $1^\circ \times 1^\circ$ and vertically within 10 m depth intervals. Binning the data at 0.1 kg m^{-3} density intervals yielded very similar results. The resulting data set included 186,880 O_2 measurements spanning 1911 to 2013 within the upper 500 m (Figure 3).

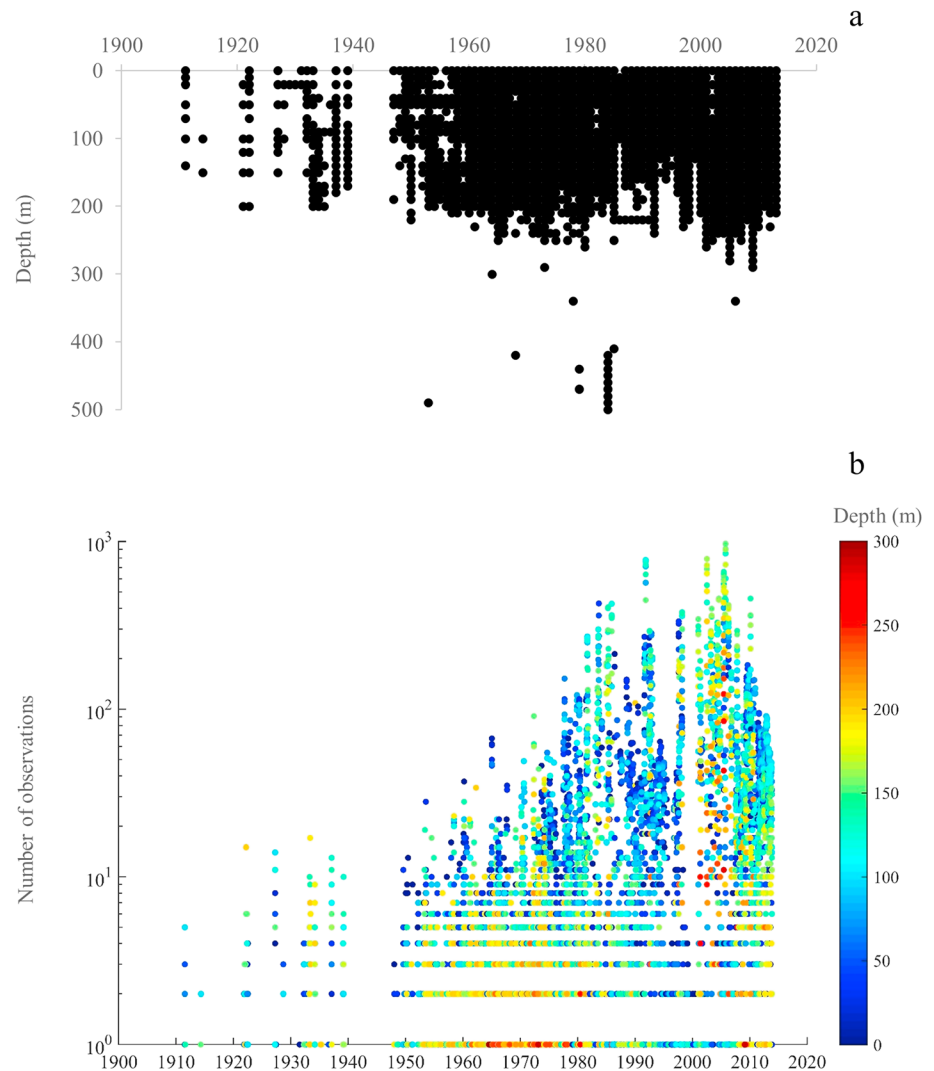


Figure 3. (a) Vertical distribution of STUW O₂ observations in the North Atlantic between 1900 and 2013. (b) Number of STUW O₂ observations in the North Atlantic for the same period. Color scale bar shows the depth of STUW O₂ observations.

NODC carries out rigorous data quality control on WOD13 data sets [Johnson *et al.*, 2013]. In this study, only accepted values from WOD13 were used (flag values of zero). Further, data quality control was conducted on WOD13 observations used for STUW O₂ trend analyses, following the approach of Jenkins and Goldman [1985]. Specifically, quality control filtering of data in this study consisted in removing observations that deviated by more than 3σ from the long-term mean (e.g., 1911–2013) at each 10 m depth interval, from surface waters down to 500 m. Flagged data under this criteria represented $\sim 1.7\%$ of the 1911–2013 (0–500 m) data set.

The vertical binning of WOD13 data allowed the assessment of temporal changes in O₂ over the entire domain of STUW by calculating monthly O₂ anomalies at individual depth horizons (10 m intervals) under the assumption that the age of the water mass at each depth horizon is similar at all sampled locations for a given year. Using this technique, we obtained time series of O₂ anomalies at individual depth layers with comparable time periods. We excluded data collected before 1950 from the analyses because of the very poor vertical and temporal (yearly) coverage (Figure 3). Data collected before 1950 were often available only for small areas of the North Atlantic and thus would bias our results. We excluded data collected below 220 m, which also exhibited poor temporal coverage. O₂ measurements below this depth were collected in less than 30% of all years between 1950 and 2013 (64 years). Observations that met these criteria represented $\sim 0.9\%$ of the 1911–2013 (upper 500 m) data set, and their exclusion resulted in a final data set composed by 185,231

observations from 28,877 casts between 1950 and 2013. On average, O_2 observations in the upper 220 m covered ~90% of the 64 years time series (Figure 3). The final data set then yielded 23 time series of STUW O_2 measurements from the surface down to 220 m (i.e., 23 depth horizons).

STUW O_2 measurements were deseasonalized by subtracting the 1950–2013 monthly mean from observed values for the corresponding month at each depth horizons as follows:

$$MO_2A(m, z) = \frac{1}{n} \sum_1^n (\text{Obs}(m, z) - \text{Mean}(m, z))$$

where MO_2A is the mean deseasonalized monthly O_2 value (mean monthly O_2 anomaly) for month m at the depth horizon z , Obs are all observed O_2 values for month m within depth layer z , Mean is the 1950–2013 average (climatological) O_2 value for month m depth layer z , and n is the number of O_2 measurements during month m at that depth horizon. Deseasonalization of O_2 observations within 10 m depth intervals was intended to minimize biases associated with vertical O_2 gradients from increasing age of STUW with depth.

Mean annual STUW O_2 anomalies (AO_2A) were then calculated for the entire domain of STUW and for specific subregions, by averaging all MO_2A values for each year, using the following equation:

$$AO_2(j) = \frac{1}{N} \sum_{i=1}^N MO_2A(i, j)$$

where j is year and N is the number of MO_2A values for the corresponding year. We also studied the AO_2A and MO_2A variability at time series stations in a similar fashion using climatological monthly values derived from the corresponding time series site (BATS: 1988–2011; Hydrostation "S": 1955–2013; CARIACO: 1996–2013; and ESTOC: 1994–2013). Unlike with WOD13 data, deseasonalization of O_2 measurements from these time series stations was not carried out using discrete depth layers because of limitations with sample size; the number of STUW O_2 observations at these sites is several orders of magnitude smaller than in WOD13 data sets. Instead, MO_2A values from the four time series stations were calculated using a common climatological monthly mean value for the entire water column for the corresponding time series station.

Linear O_2 trends were calculated for each of the time series stations and the selected subregions using least squares linear regression analysis. Time periods for linear regression analysis from time series stations were 1996–2013 for CARIACO, 1988–2011 for BATS, 1980–2013 for Hydrostation "S", and 1994–2013 for ESTOC. Specifically, we estimated linear O_2 trends over the 1980–2013 period within subregions of $5^\circ \times 5^\circ$ using AO_2A values from the western North Atlantic near the BATS and Hydrostation "S" stations and the eastern North Atlantic near the ESTOC station (i.e., BATS: $30\text{--}35^\circ\text{N}$, $60\text{--}65^\circ\text{W}$ and ESTOC: $25\text{--}30^\circ\text{N}$, $15\text{--}20^\circ\text{W}$). The O_2 trend for this period was also calculated in a larger subregion in the southeastern Caribbean Sea near the CARIACO station ($5^\circ \times 10^\circ$; $10\text{--}15^\circ\text{N}$, $60\text{--}70^\circ\text{W}$). We chose a larger area in the southeastern Caribbean Sea to compensate for the lower spatial and temporal data coverage in this subregion compared to the eastern and western North Atlantic subregions. The linear O_2 trend between 1980 and 2013 was also calculated for the entire domain of STUW.

2.3. Satellite Sea Surface Temperature Within STUW Formation Regions

Mean monthly and annual satellite sea surface temperature (SST) anomalies in the area of formation of STUW were examined to quantify possible SST trends over the last three decades (1982–2012 inclusive). The areal extent of the formation region of STUW varied up to an order of magnitude between July–December and January–June periods [O'Connor *et al.*, 2005]. We constructed time series of mean SST anomalies from spatially varying STUW formation regions defined using the WOA09 North Atlantic θ and S seasonal and annual objectively analyzed climatologies. WOA09 seasonal climatologies are based on mean fields calculated for January–March (winter), April–June (spring), July–September (summer), and October–December (fall) periods [see Locarnini *et al.*, 2010]. The regions were defined by outlining the area of all locations (grid cells) where STUW was detected at the surface (0–10 m) using a $1^\circ \times 1^\circ$ linear interpolation.

Specifically, a time series of daily SST observations spanning 1982 to 2012 (inclusive) was extracted from the Advanced Very High Resolution Radiometer Pathfinder version 5.2 (PFV5.2). These data were averaged into monthly mean periods. A monthly climatology was also computed. The nominal spatial resolution of these data is $4 \times 4 \text{ km}^2$ per pixel. The data were obtained from the U.S. National Oceanographic Data Center

(NODC) and the Group for High Resolution Sea Surface Temperature (<http://pathfinder.nodc.noaa.gov>) [Casey *et al.*, 2010]. The PFV5.2 data set has a gap, from 2 October 1994 to 17 January 1995. Monthly SST values were deseasonalized by subtracting the climatological monthly value from the mean SST observed within the seasonal region of formation for the corresponding month. Linear trends of SST anomalies over time (months) were then calculated for each of the formation regions using least squares linear regression.

2.4. Climate Indices

The North Atlantic Oscillation (NAO) and the Atlantic Multidecadal Oscillation (AMO) climate indices were used since these are considered to be the dominant climate controls over the North Atlantic region [Hurrell, 1995, 1996; Visbeck *et al.*, 1998; Marshall *et al.*, 2001; Gruber *et al.*, 2002; Johnson and Gruber, 2007; Schlesinger and Ramankutty, 1994; Kerr, 2000; Enfield *et al.*, 2001]. To study possible relationships between STUW O₂ and climate forcing over the North Atlantic Ocean, we conducted cross-correlation analyses between the NAO and AMO indices and STUW O₂ anomalies using time lags spanning from 0 to 8 years. The NAO index is a metric of sea level atmospheric pressure anomalies between the Azores High and the Icelandic Low pressure systems [Barnston and Livezey, 1987]. The AMO index is a multidecadal mode of variability of SST anomaly in the North Atlantic region (0–60°N) that oscillates with a period of 65–75 years [Schlesinger and Ramankutty, 1994; Kerr, 2000; Enfield *et al.*, 2001], although higher-frequency cycles of 20–40 years have also been reported [Goldenberg *et al.*, 2001; Vincze and Janosi, 2011]. Periods of positive NAO index phase, which exhibit high trade winds and westerlies intensity, typically show colder-than-normal SST and therefore coincide with the negative AMO index phase [Enfield *et al.*, 2001; Gruber, 2009; Visbeck *et al.*, 2013]. Monthly NAO and AMO index data were retrieved from the NOAA National Centers for Environmental Prediction (NCEP). NCEP's NAO index values are normalized using the 1981–2010 base period monthly means and standard deviations.

3. Results

Average spatial and vertical distributions of STUW in the North Atlantic are shown in Figure 1. STUW forms in the eastern subtropical North Atlantic at the surface to the southwest and northwest of the Canary Islands [also see Doney *et al.*, 1998; Qu *et al.*, 2013; Shcherbina *et al.*, 2015]. STUW may also outcrop in the central subtropical North Atlantic and around Bermuda (see Figure 1). STUW sinks as it spreads to the western tropical North Atlantic including the Caribbean Sea, where it reaches average depths of ~250–300 m west of Puerto Rico and around Cuba.

The O₂ in STUW follows a gradient, with highest concentrations (~230 μmol kg⁻¹) in the area of water mass formation near the surface and lowest (~160 μmol kg⁻¹) where it is deepest in the west (Figure 4, top). This is consistent with cumulative apparent oxygen utilization (AOU), the result of remineralization of sinking organic matter as the water mass spreads across the Atlantic. STUW is also thickest (~80 to 100 m) in the eastern subtropical North Atlantic near the area of formation and thinnest (~10 to 20 m) south of 20°N (Figure 4, middle). The total estimated STUW O₂ stock is ~105 × 10¹² mol O₂, with ~80% of this distributed across the northeastern and northern portions of the North Atlantic subtropical gyre (20°–40°N, 10°–80°W; Figure 4).

4. Annual STUW O₂ Anomalies (AO_{2A})

Time series of AO_{2A} computed using data collected at the CARIACO (1996–2013), BATS (1988–2011), and Hydrostation "S" (1980–2013) showed negative linear trends (rates of -0.71, -0.28, and -0.37 μmol kg⁻¹ yr⁻¹, respectively; Figure 5 and Table 2). The interannual variability of AO_{2A} at CARIACO was higher than that observed at BATS and Hydrostation "S". AO_{2A} at ESTOC did not show a trend.

To assess whether the observed trends in AO_{2A} measured at the time series sites were comparable to changes at broader spatial scales, we examined historical WOD13 records for changes in AO_{2A} across three larger regions in the North Atlantic (Figure 6). Based on these AO_{2A} observations, we found that STUW O₂ declined at a rate of -0.58 μmol kg⁻¹ yr⁻¹ in the southeastern Caribbean Sea (Region 1 in Figure 6) and -0.68 μmol kg⁻¹ yr⁻¹ in the western subtropical North Atlantic (Region 2) between 1980 and 2013 (Table 2). Declining rates of STUW O₂ at CARIACO and those estimated for the subregion in the Caribbean Sea are comparable. The rate of STUW O₂ loss measured at BATS and Hydrostation "S" is ~58 and 46% lower than that estimated in Region 2, respectively. As in ESTOC, a trend in STUW O₂ loss was not detected in

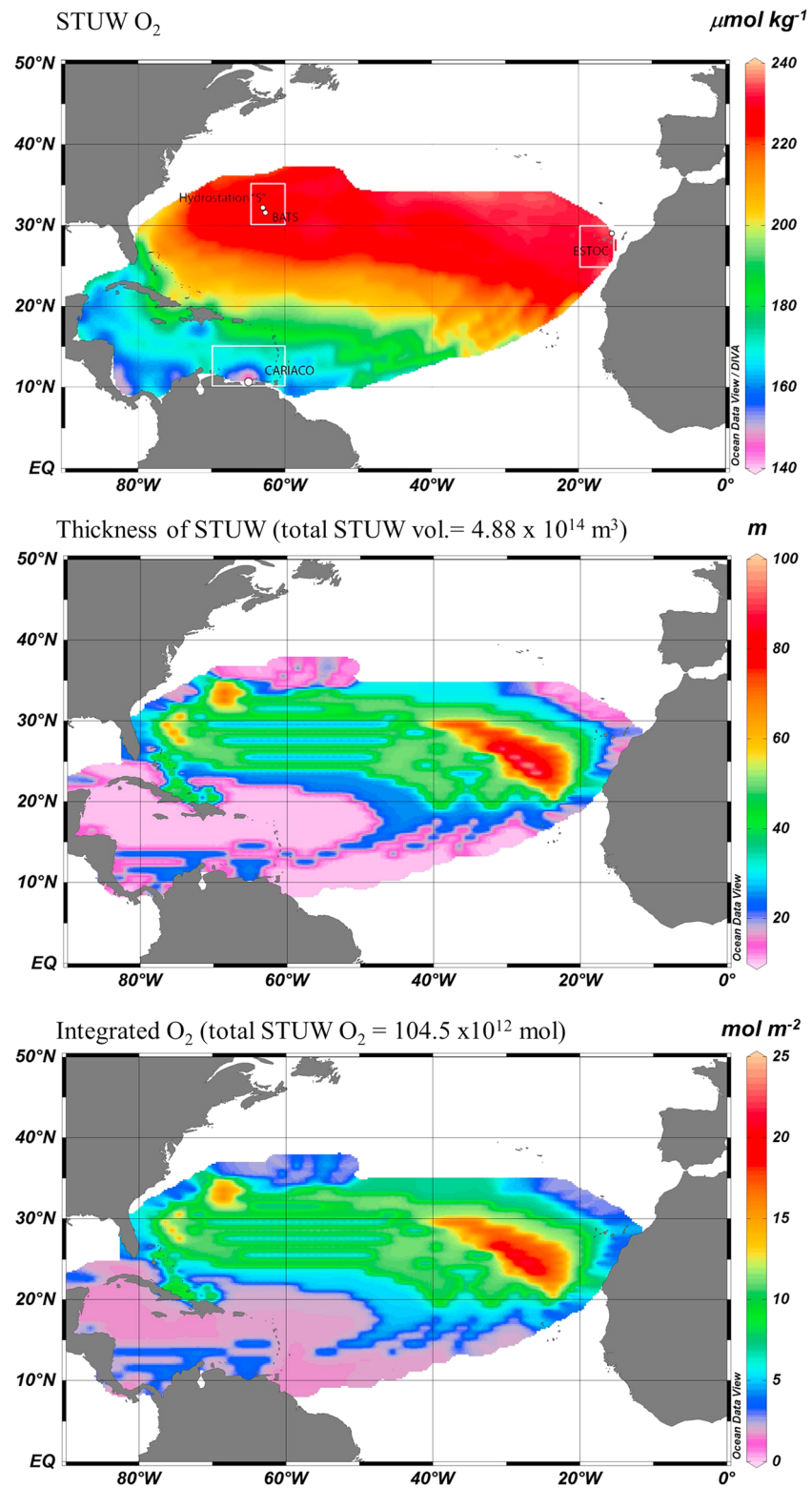


Figure 4. (top) Annual average distribution of STUW O₂ concentration. White circles indicate the location of time series stations, and white rectangles indicate subregional domains of corresponding time series station. (middle) STUW thickness. (bottom) O₂ integrated over the thickness of the STUW at individual 1° × 1° grid cells. The value within parentheses in Figure 4 (bottom) indicates the STUW O₂ standing stock.

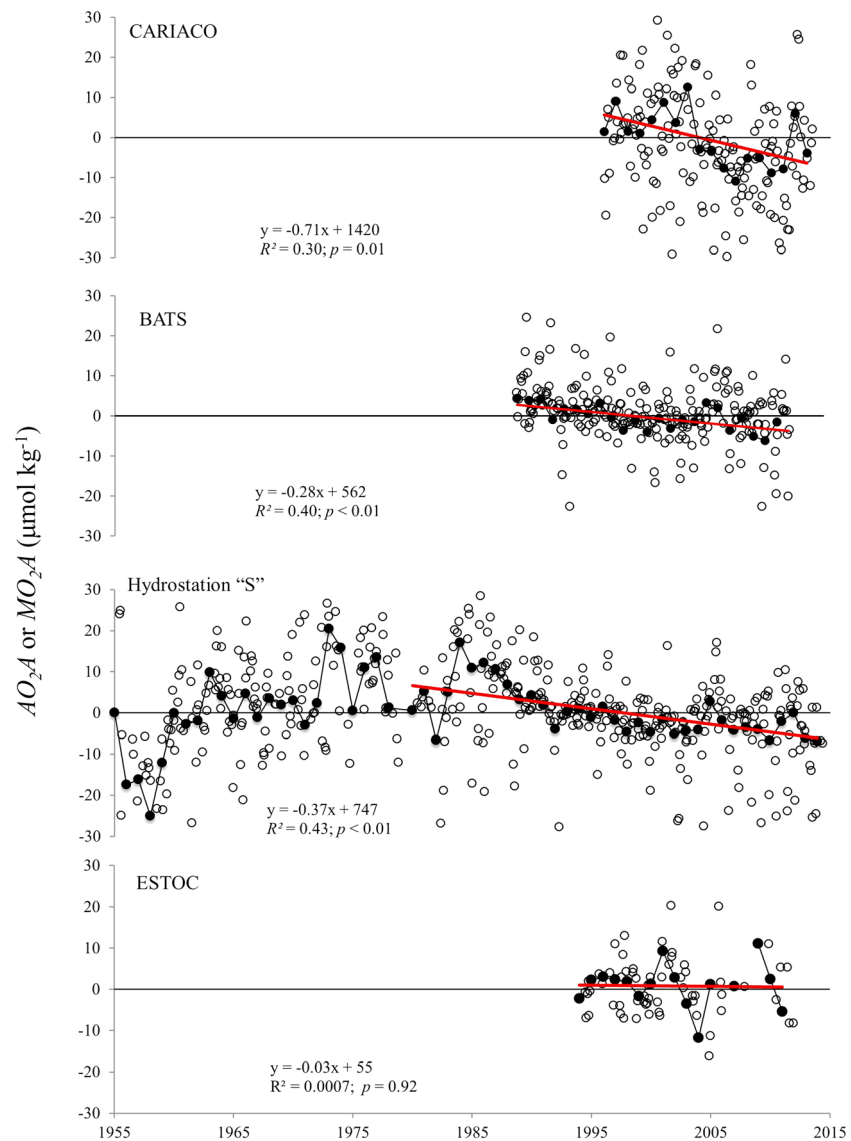


Figure 5. Mean annual and monthly STUW O₂ anomalies (AO_{2A} (filled circles) and MO_{2A} (open circles), respectively) measured at the four time series sites. The red line indicates the linear regression for annual mean values (CARIACO: 1996–2013; BATS: 1988–2011; Hydrostation "S": 1980–2013; and ESTOC: 1994–2013). Equations, coefficients of determination (R^2), and p values of all linear regressions are shown for each plot.

Region 3, the eastern subtropical North Atlantic, over the same period. The rate of STUW O₂ loss calculated for the entire domain of STUW during the 1980–2013 period is $-0.75 \mu\text{mol kg}^{-1} \text{yr}^{-1}$, which is comparable to those from Regions 1 and 2 (Table 2).

4.1. SST Trends in the Formation Region of STUW

The climatological area of STUW formation in the eastern subtropical North Atlantic between $\sim 20^\circ\text{N}$ and 30°N varies significantly between seasons (Figure 7, left column). Specifically, the average surface area of STUW formation in the summer-fall period is $\sim 5.8 \times 10^{11} \text{ m}^2$, and it grows to $\sim 2.4 \times 10^{12} \text{ m}^2$ during winter-spring. The difference between spring and summer formation regions is $\sim 1.8 \times 10^{12} \text{ m}^2$, which is in good agreement with that derived by O'Connor *et al.* [2005] ($1.7 \times 10^{12} \text{ m}^2$).

In terms of temperature, SST within the formation region of STUW increased at an average rate of $\sim 0.035^\circ \text{Cyr}^{-1}$, or over 1°C , between November 1982 and December 2013 (Figure 7, right column). This rate of

Table 2. Time Periods Used for Corresponding STUW O₂ Time Series Analyses, STUW O₂ Rate of Change (dO₂/dt) and Corresponding Coefficient of Correlation (R²), Standard Deviation (SD), and *p* Value^a

	Trend Period	dO ₂ /dt μmol kg ⁻¹ yr ⁻¹	R ² (SD)	<i>p</i> Value	ΔO ₂ μmol kg ⁻¹
CARIACO	1996–2013	-0.71	0.30 (0.27)	= 0.01	-23.4
BATS	1988–2011	-0.28	0.40 (0.08)	< 0.01	-9.2
Hydrostation "S"	1980–2013	-0.37	0.43 (0.08)	< 0.01	-12.2
ESTOC	1994–2013	-0.03	0.0007 (0.26)	0.92	No O ₂ loss
Average		-0.45			-15.0
SD		0.23			7.5
Region 1	1980–2013	-0.58	0.34 (0.18)	< 0.01	-19.1
Region 2	1980–2013	-0.68	0.43 (0.14)	< 0.01	-22.4
Region 3	1980–2013	0.006	0.0001 (0.12)	0.96	No O ₂ loss
Average		-0.63			-20.8
SD		0.07			2.3
All STUW	1980–2013	-0.75	0.44 (0.15)	< 0.01	-24.8

^aAlso shown is the estimated STUW O₂ loss (ΔO₂) between 1980 and 2013 using the corresponding rate of change observed at the four time series sites and regionally. Regions 1–3 are the same as in Figure 6.

increase was highest in summer (0.040°C yr⁻¹) and lowest in winter (0.027°C yr⁻¹). The mean STUW *S* also increased between 1980 and 2013, on average 0.063 salinity units (0.0019 yr⁻¹). An increase in *S* is also observed at Hydrostation "S" and BATS over the course of these time series (Figure 2). This is consistent with the results from previous studies showing an increase in *S* in the subtropical North Atlantic over the last 50 years from increasing excess evaporation over precipitation, associated in turn with shifts in El Niño–Southern Oscillation and Pacific Decadal Oscillation conditions [Curry *et al.*, 2003; Gordon and Giulivi, 2008]. A decreasing *S* trend, however, is observed in the CARIACO station that appears to be associated with increasing precipitation in the southern Caribbean [Lorenzoni, 2012].

5. Discussion

5.1. Variability of North Atlantic STUW O₂

The initial amount of O₂ within a particular water mass, also known as preformed oxygen (O₂^{sat}), is mainly determined by thermodynamic equilibrium with the atmosphere when the water mass is at the surface. After subduction and mixing with other water masses, a water parcel may lose O₂ progressively along its circulation path. An important nonconservative process of O₂ loss in the ocean is respiration of organic matter. The amount of O₂ consumed by respiration, or AOU, is usually expressed as the difference between saturation and measured O₂ levels (AOU = O₂^{sat} - O₂^{measured}); this property is modulated by physical (diffusion, circulation, and ventilation) and biological processes (productivity and respiration or remineralization) [Deutsch *et al.*, 2005]. Changes in total O₂ in a water mass over time (ΔO₂) are therefore determined by changes in O₂^{sat} and AOU as

$$\Delta O_2 = \Delta O_2^{\text{sat}} + \Delta \text{AOU}$$

The extent to which ΔO₂ is impacted by changes in (1) solubility and (2) the combined effects of ventilation, transport, and biological processes can be estimated independently by examining changes in O₂^{sat} and AOU based on observations of *θ*, *S*, and in situ O₂. The solubility equations of Garcia and Gordon [1992] provide a means to estimate changes in ΔO₂^{sat} given *θ* and *S* change in the area of formation of STUW. Within the STUW, subsequent changes in *θ* and *S* are expected to be conservative and, by definition of the water mass, do not change significantly within the STUW.

During formation of STUW, O₂ levels in this water mass should be mostly driven by changes in solubility and wind-driven mixing and ventilation since it is in direct contact with the atmosphere and within the mixed layer. The effect of respiration on O₂ levels due to remineralization of export production is likely minimal near the surface compared to physical drivers. SST in the region of STUW formation increased ~1°C between 1982 and 2013 (Figure 7). Similar increases in SST have been reported for other areas of the North Atlantic [Enfield and Mestas-Nunez, 1999; Chollett *et al.*, 2012; González Taboada and Anadón, 2012; Pörtner *et al.*, 2014; Muller-Karger *et al.*, 2015]. Sustained increase in North Atlantic STUW salinity has also

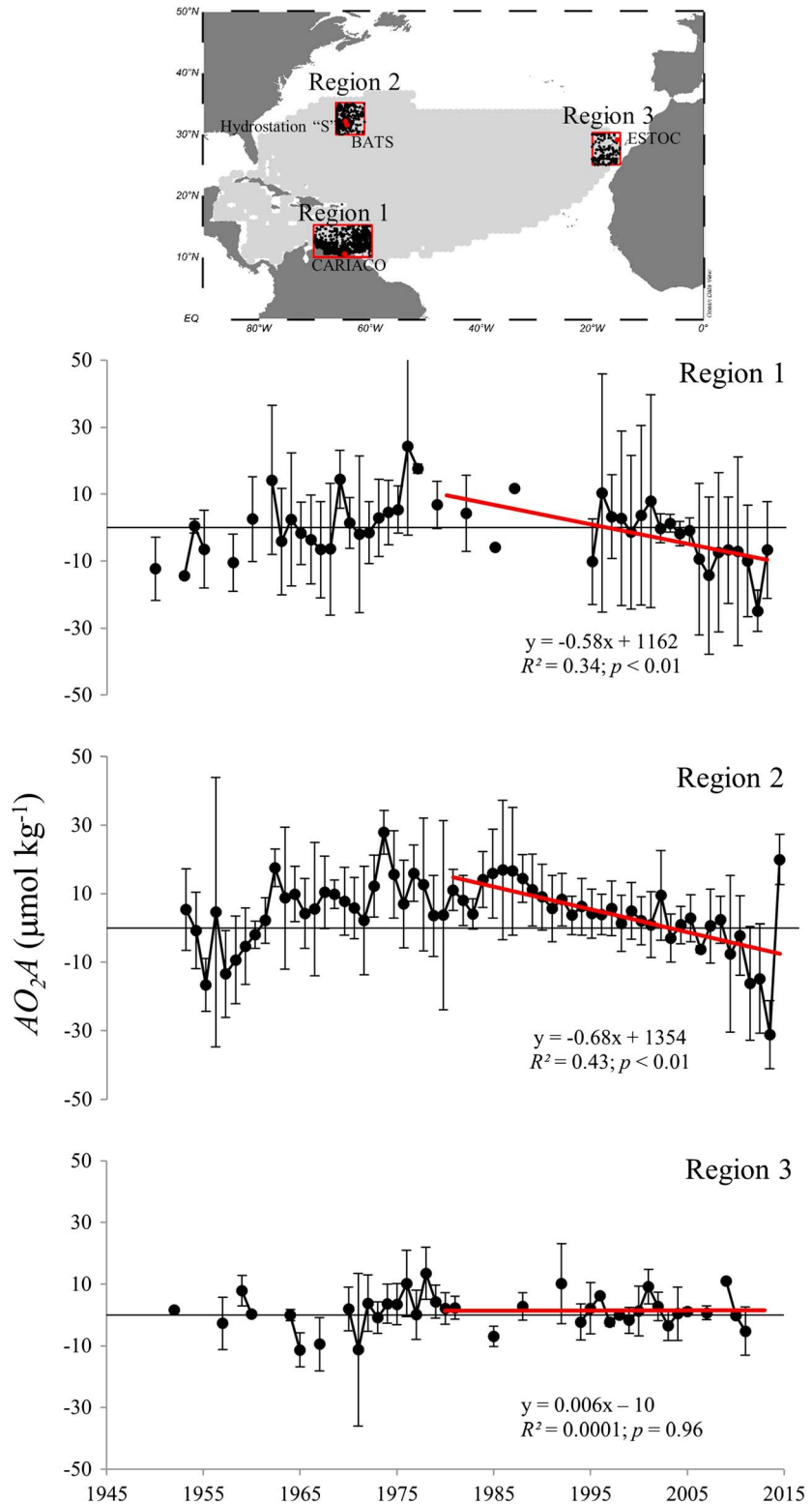


Figure 6. Mean annual STUW O₂ anomaly (AO_{2A}) with respect the 1950–2013 mean value extracted from a 10° × 5° area in the southeastern Caribbean Sea (Region 1) and 5° × 5° area in the western and eastern North Atlantic subtropical gyre (Regions 2 and 3, respectively). Black dots on maps indicate locations from which data were collected. Red dots on map show the location of each time series station. The domain of STUW is shown in grey. The red line indicates the linear O₂ trend between 1980 and 2013, and error bars show one standard deviation. Equations, coefficients of determination (*R*²), and *p* values of all linear regressions are shown for each plot.

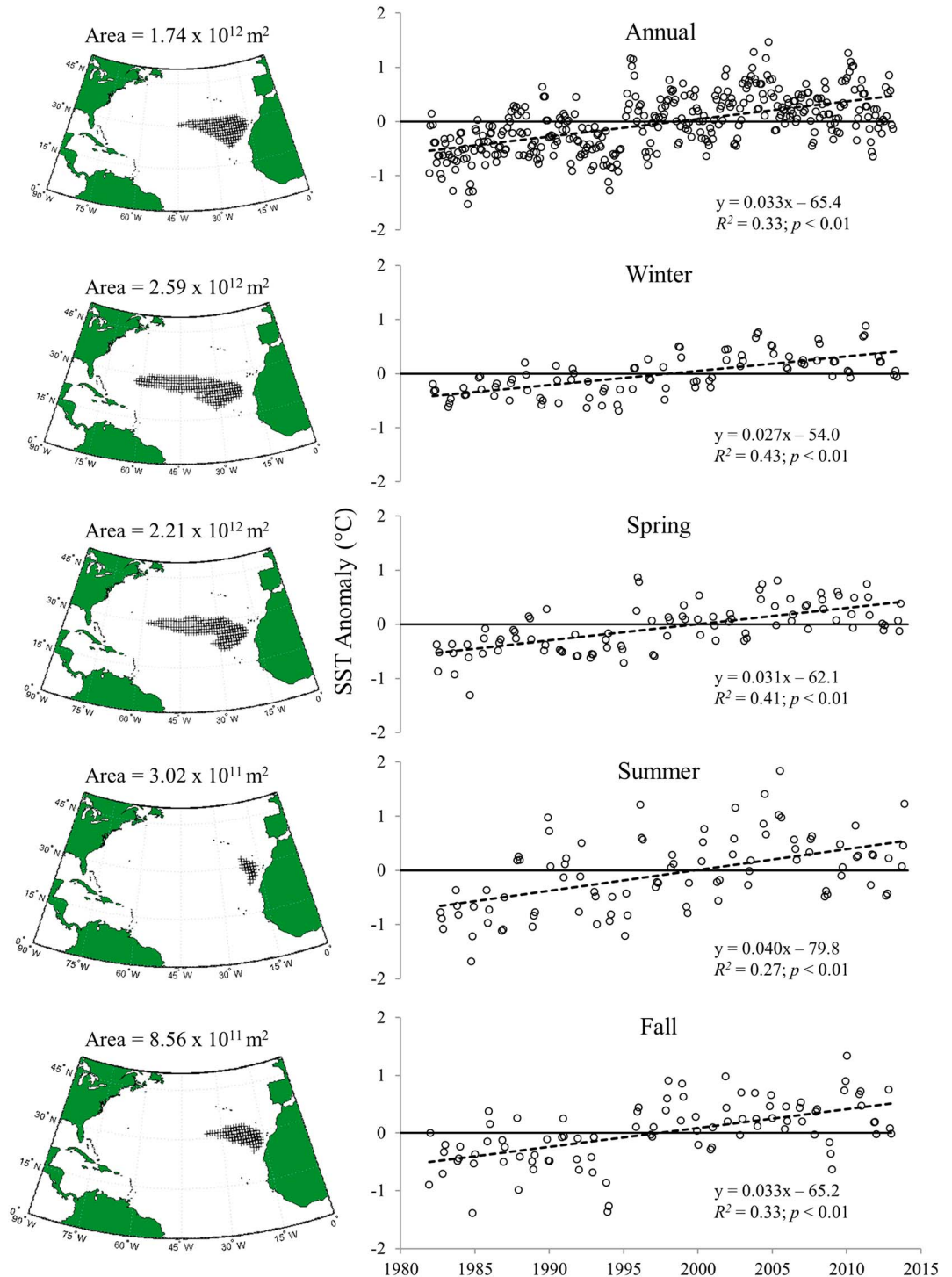


Figure 7. (left column) Climatological annual and seasonal formation regions of STUW. Seasonal climatologies are derived from mean fields for January–March (winter), April–June (spring), July–September (summer), and October–December (fall) periods. Climatological areal extent of formation regions are indicated for each period. (right column) Trends of mean SST anomalies between 1982 and 2013 within the formation region for the corresponding season. Dashed black lines indicate the SST trend between 1982 and 2013. Coefficients of determination (R^2) and p values of all linear regressions are shown.

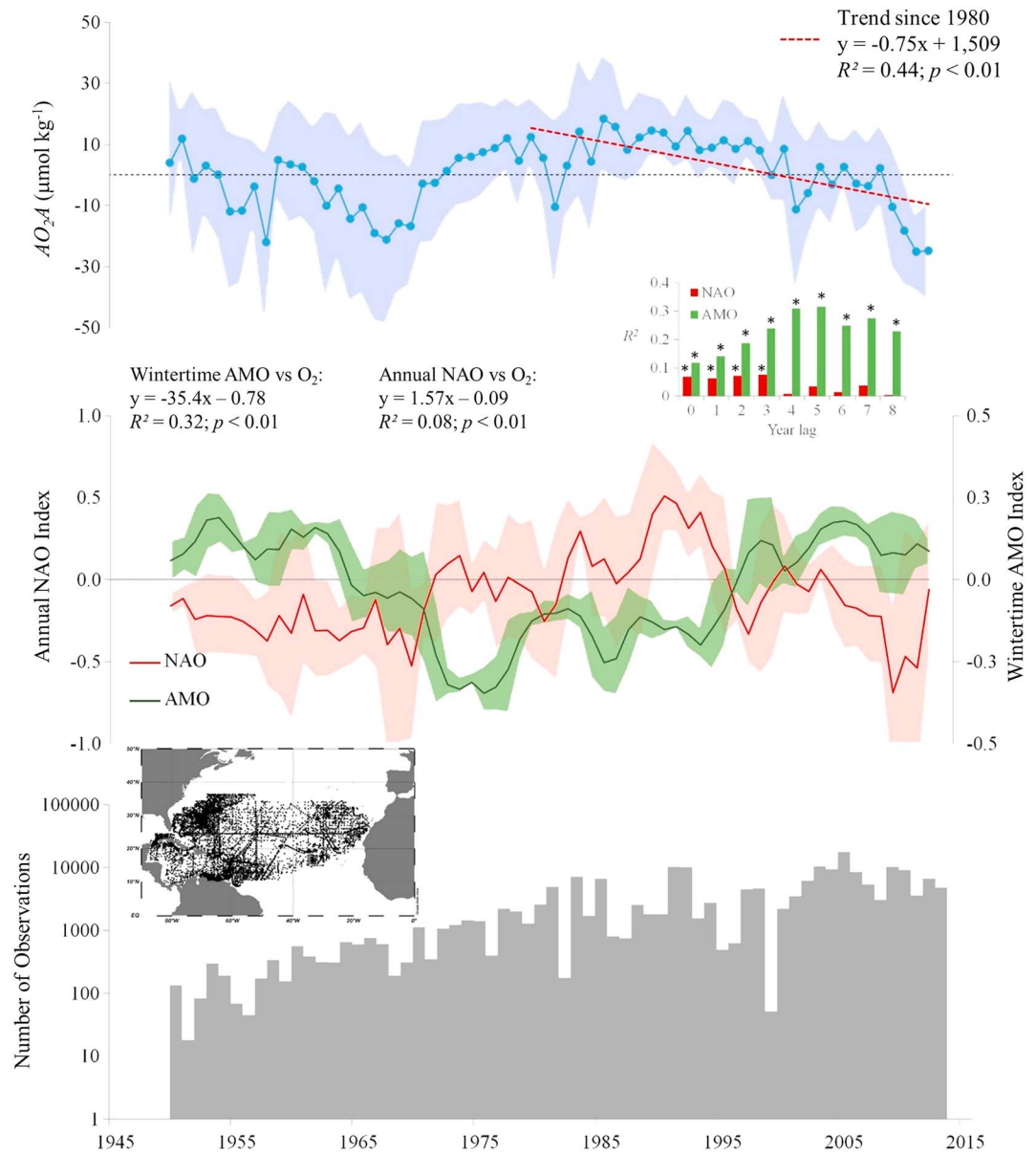


Figure 8. (top) Mean annual STUW O_2 anomaly (AO_{2A} ; blue curve with one standard deviation envelope) with respect to the 1950–2013 mean value. The red line indicates the linear O_2 trend between 1980 and 2013. (middle) Three year smoothed mean annual NAO (red curve) and wintertime (January–March) AMO (green curve) indices with one standard deviation envelopes. Histogram located between Figure 8 (top) and Figure 8 (middle) shows correlation coefficient (R^2) values yielded by linear regressions between each index and O_2 anomalies at 0 to 8 years positive lags, and asterisks indicate correlations that are statistically significant. Equations, R^2 , and p values are shown for the linear regressions between each climate index and O_2 anomalies with 3 and 5 years positive lags for the NAO and wintertime AMO, respectively. (bottom) The number of STUW O_2 observations throughout the study period. Dots on map indicate locations from which data were collected.

been noted previously [Hurrell, 1995; Curry *et al.*, 2003] and has been attributed to increased evaporation over the North Atlantic region. In this study we found that the mean STUW S has increased at 0.0019 year^{-1} between 1980 and 2013. The observed increase of $\sim 1^\circ\text{C}$ in SST and 0.063 in S (using an estimated S increase rate of 0.0019 year^{-1} over a 33 year period) in the region of formation of STUW between 1980 and 2013 would result, on average, in an O_2^{sat} decrease of $3.3 \mu\text{mol kg}^{-1}$ ($\Delta O_2^{\text{sat}} = O_{2013}^{\text{sat}} - O_{1980}^{\text{sat}}$) within this region over this period. This simple empirical estimate is derived from using, for example, SST and S values at the beginning and end of our time series. Specifically, end-member SST and S values of 21.5°C and 36.780 were used to calculate the O_2^{sat} in 1980 ($222.6 \mu\text{mol kg}^{-1}$) and 22.5°C and 36.843 ($36.780 + 0.063$) for O_2^{sat} in

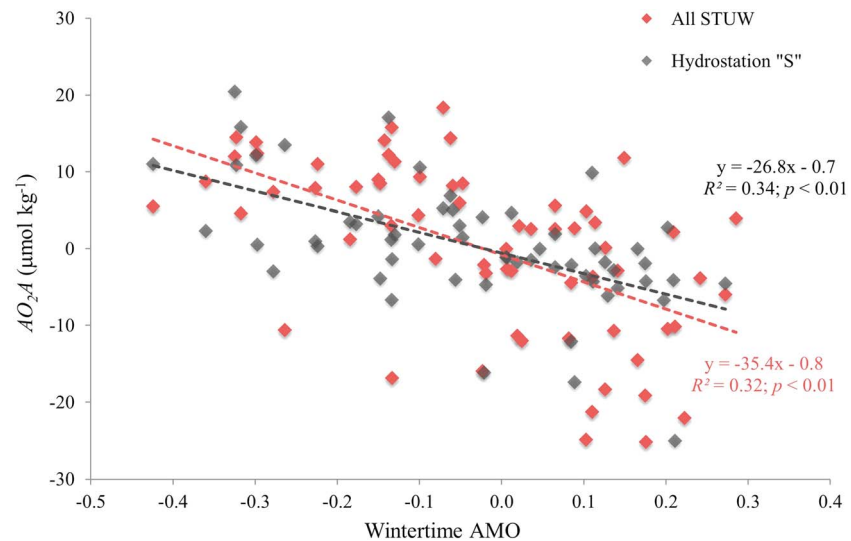


Figure 9. Mean annual STUW O_2 anomaly (AO_2A) versus wintertime (January–March) Atlantic Multidecadal Oscillation index values with a 5 year positive lag for AO_2A from all observations within the entire climatological domain (all STUW; red diamonds) and a 0 year lag for AO_2A from Hydrostation S (grey diamonds). Equations, coefficients of determination (R^2), and p values of linear regressions are shown with the corresponding color.

2013 ($219.3 \mu\text{mol kg}^{-1}$). Increasing S and warming of STUW by $\sim 1^\circ\text{C}$ in its region of formation should have led to a decline in O_2 solubility of $\sim 3 \mu\text{mol kg}^{-1}$ in the last 33 years. Therefore, thermodynamic changes could only account for an $\sim 10\%$ of the observed O_2 loss of $\sim 25 \mu\text{mol kg}^{-1}$ in STUW, at least over the period 1980 to 2013. If solubility does not appear to be a major driver in the loss of STUW O_2 since 1980, declining O_2 in this water mass over this period must therefore result from (1) increasing respiration rates within subsurface layers, (2) increasing accumulation of AOU below the surface due to slowdown of STUW formation and transport rates, or (3) decreasing wind-driven ventilation within and immediately below the mixed layer. The observed STUW O_2 loss, however, is likely the result of the combined effects of these processes.

A steady increase in organic matter export rates over the STUW domain would have enhanced O_2 removal proportionally by stimulating microbial respiration at depths below the mixed layer depth [Redfield, 1934]. However, sediment trap data from BATS [Lomas *et al.*, 2010, 2013] and CARIACO [Taylor *et al.*, 2012; Scranton *et al.*, 2014] show that annual export production has not changed over the course of these time series, suggesting that respiration rates in the North Atlantic have remained constant since the late 1980s, under the assumption that export fluxes measured at these two time series stations are representative of the regional North Atlantic. Other studies based on observations and numerical models have also found that O_2 loss in the Atlantic and Pacific basins is mainly driven by physical processes rather than changes in respiration [Bopp *et al.*, 2002; Keeling and García, 2002; Deutsch *et al.*, 2005; Helm *et al.*, 2011]. Thus, the observed O_2 decline between 1980 and 2013 is most likely the result of changes in physical forcing controlling STUW formation and transport rates and ventilation in the formation region and areas where STUW is within or near the base of the mixed layer (i.e., upper ~ 100 m; see Figure 1).

STUW formation and transport rates are the result of a complex interplay between wind-driven SST cooling and deepening of the mixed layer, air-sea fluxes (i.e., the balance between evaporation and precipitation), submesoscale (1–10 km) “slumping” of high-density water induced by baroclinic mixed layer instabilities, and large-scale circulation dynamics [O’Connor *et al.*, 2005; Qu *et al.*, 2013; Shcherbina *et al.*, 2015]. High wind stress conditions in the formation region of STUW (eastern and central North Atlantic; see Figure 7), and thus high STUW outcropping and transport rates, should lead to less AOU buildup in STUW due to faster transit of the water mass across the basin; faster circulation should lead to less exposure of STUW to microbial respiration along its circulation path. The opposite is expected to occur during periods of low wind intensity, with lower outcropping of STUW and transport rates. Under these conditions, higher AOU accumulation rates are expected due to slower transport of STUW toward the west, and a negative O_2 trend would result in areas outside the formation region. Varying wind stress conditions also affect

ventilation of subsurface STUW isopycnals (after subduction) in regions where STUW is within the mixed layer or immediately below it. STUW is a relatively shallow water mass and thus particularly sensitive to ventilation; STUW is present in the upper 100 m over ~60% of its climatological domain (Figure 1). Periods of low wind stress conditions, and therefore poor ventilation of STUW, would also lead to accumulation of AOU and negative O_2 trends if these conditions were sustained over time. These two processes could, in part, explain the steeper negative trend detected at CARIACO, as compared to those from BATS and Hydrostation "S". STUW reaching CARIACO is older and probably carries a stronger AOU buildup signal than at the two sites near Bermuda.

We observed decadal-scale variability in STUW O_2 . In the North Atlantic, long-term air-sea fluxes of heat, salt, and buoyancy follow variability that can be tracked using the NAO and AMO indices [Hurrell, 1995, 1996; Visbeck *et al.*, 1998; Marshall *et al.*, 2001; Gruber *et al.*, 2002; Goldenberg *et al.*, 2001; Enfield *et al.*, 2001; Vincze and Janosi, 2011]. O_2 inventories within North Atlantic mode water also follow shifts in the NAO index [i.e., Johnson and Gruber, 2007]. During the positive phase of the NAO, which corresponds to a high-pressure gradient between the Azores and Iceland pressure systems, westerly winds are stronger and are displaced northward of 45°N, and the trade winds are also more intense between 10°N and 30°N [Gruber, 2009; Visbeck *et al.*, 2013]. This affects water mass formation and ventilation of mode waters, especially during winter months. Shifts in the NAO phase, however, affect wind patterns across the North Atlantic differently. For example, during a strong positive NAO phase, the thickness of Subtropical Mode Water (or 18°C water) is reduced due to smaller negative buoyancy fluxes at the ocean's surface resulting from anomalously high wintertime SST and reduced mixing in the western subtropical North Atlantic [Visbeck *et al.*, 2013; Gruber *et al.*, 2002]. The opposite occurs in the Labrador Sea [Visbeck *et al.*, 2013], where formation rates of Subpolar Mode Waters and O_2 inventories are positively correlated to the NAO phase [Johnson and Gruber, 2007; Stendardo and Gruber, 2012]. Increased wind strength and decreased SST in the tropical North Atlantic during positive NAO phases in turn stimulate subduction and ventilation of waters masses in this region [Marshall *et al.*, 2001; Visbeck *et al.*, 2013].

We found a weak positive correlation ($R^2 = 0.08$; $p < 0.05$) between the mean annual NAO index and AO_2A between 1950 and 2013 (Figure 8). However, a significantly higher negative correlation ($R^2 = 0.32$; $p < 0.01$) between wintertime (January–March) AMO index and AO_2A was observed for the entire domain of STUW and from observations at Hydrostation "S" (Figure 9). STUW O_2 values were below the climatological mean between 1950 and the early 1970s and after the mid-1990s, when wintertime AMO (NAO) was in a positive (neutral-negative) phase. They shifted above the climatological mean between the early 1980s and the mid-1990s, when wintertime AMO (NAO) was in a negative (positive) phase. AOU values showed the opposite pattern, with high values during the positive (negative) wintertime AMO (NAO) phase. During the wintertime AMO– (NAO+) phase, wintertime SST in the North Atlantic is colder than normal and the intensity of the trade winds is high [Cayan, 1992; Enfield *et al.*, 2001; Marshall *et al.*, 2001; Visbeck *et al.*, 2013]. These conditions lead to increased STUW production and subduction rates in the eastern subtropical and tropical North Atlantic and thus lower AOU buildup in STUW if indeed export productions have remained constant during this period. Wintertime AMO– (NAO+) conditions also lead to higher O_2 concentrations within STUW as a result of increased gas solubility in surface waters and enhanced mixing and ventilation in both the formation region of STUW (Figure 7) and in subsurface STUW isopycnals, i.e., where STUW is within or near the base of the mixed layer. The mean rate of change of STUW O_2 over the entire domain of this water mass calculated between 1980 and 2013 ($-0.75 \mu\text{mol kg}^{-1} \text{yr}^{-1}$; Table 2) is consistent with previously reported thermocline O_2 declines in the North Atlantic and North Pacific basins of 0.3 and $0.7 \mu\text{mol kg}^{-1} \text{yr}^{-1}$ over the last 50 years [Whitney *et al.*, 2007; Keeling *et al.*, 2010; Stendardo and Gruber, 2012]. In particular, this O_2 loss rate is comparable to long-term O_2 declines of $\sim 0.3\text{--}0.5 \mu\text{mol kg}^{-1} \text{yr}^{-1}$ within mode and intermediate waters observed in the eastern and northern North Atlantic since 1960, which have also been attributed to NAO-driven changes in ventilation [Stendardo and Gruber, 2012].

5.2. Detection of STUW O_2 Trends at Time Series Stations

While negative trends in AO_2A were detected at the BATS, Hydrostation "S", and CARIACO stations over the course of these time series, no apparent change in AO_2A was observed at ESTOC (Figure 5). ESTOC is located on the eastern edge of the STUW formation region (Figure 1). The hydrography at the ESTOC site changes because this is at the edge of the North Atlantic gyre circulation, and therefore, the site alternately experiences the effects of the African upwelling system and the gyre, depending on season and interannual variations. In this study we found that STUW is observed at ESTOC only in summer and fall (Figure 2) as a result of

the seasonal increase in water column temperature. Due to the proximity of ESTOC to the formation region of STUW, variability in STUW O_2 at this site should be mainly controlled by in situ changes in air-ocean thermodynamic equilibrium and upper ocean turbulence. While STUW is at the surface, STUW O_2 should be near atmospheric equilibrium. Although SST has increased at $0.035^\circ\text{C yr}^{-1}$ within the formation region of STUW since 1982 (Figure 7), a sustained decline in STUW O_2 was not yet detectable using ESTOC observations. In part, this may be due to the lack of a clear positive trend in SST in this region since the onset of the ESTOC time series (1994), especially during spring, summer, and fall (Figure 7). Furthermore, the absence of a declining trend in STUW O_2 at ESTOC could be due to the variability in the data, but also because ESTOC is at the edge of the STUW region of formation, and therefore, ESTOC is sporadically within the STUW formation region. The frequency of detection of STUW at ESTOC decreased from an average of $5.3 \text{ months yr}^{-1}$ during 1994–2002 to $2.4 \text{ months yr}^{-1}$ during 2003–2011, which is likely a data artifact resulting from decreased sampling frequency at ESTOC since 2004.

Interannual variability in AO_2A observed at CARIACO (Figure 5) is in part due to changing upwelling conditions in the southeastern Caribbean Sea. In the southern Caribbean Sea, STUW shoals to the surface between January and April due to coastal upwelling. This upwelling injects nutrients into the euphotic zone and stimulates high rates of primary production, leading to rates of $350\text{--}600 \text{ g C m}^{-2} \text{ yr}^{-1}$ [Muller-Karger *et al.*, 2001; Rueda-Roa and Muller-Karger, 2013; Muller-Karger *et al.*, 2013]. The strength and duration of upwelling events, and thus the presence of STUW at or near the surface in this location, are controlled by the intensity of the trade winds and the intensity of the geostrophic Caribbean Current [Muller-Karger *et al.*, 2001; Astor *et al.*, 2003]. STUW O_2 levels at CARIACO are the result of the complex interaction between (1) local diffusive air-ocean gas exchange and upper ocean turbulence (ventilation when the STUW reaches the surface), (2) O_2 production by photosynthetic carbon fixation, and (3) respiration of sinking and suspended particulate and dissolved organic carbon. If primary production is balanced by respiration in the upper $\sim 100 \text{ m}$, STUW O_2 levels are then largely controlled by ventilation associated with changes in upwelling strength and vertical mixing. The changes observed in STUW O_2 at CARIACO are consistent with this mechanism, as weaker upwelling events would reduce the effective ventilation of this water mass. Indeed, between 1996 and 2003, when trade winds were strong ($>6 \text{ m s}^{-1}$) [Taylor *et al.*, 2012], there was a predominance of positive AO_2A (Figure 5). Since 2004, significant reductions in upwelling strength and in trade winds intensity occurred associated with a slight northward shift in the average position of the Intertropical Convergence Zone [Taylor *et al.*, 2012; Scranton *et al.*, 2014]. This period was characterized by the predominance of negative AO_2A at CARIACO (Figure 5). Overall, CARIACO data show that a STUW O_2 loss ($-0.71 \mu\text{mol kg}^{-1} \text{ yr}^{-1}$) is $\sim 18\%$ higher than that measured regionally (Region 1; $-0.58 \mu\text{mol kg}^{-1} \text{ yr}^{-1}$) and slightly lower than that for the total STUW trends ($-0.75 \mu\text{mol kg}^{-1} \text{ yr}^{-1}$). A lower STUW O_2 loss trend in the regional southern Caribbean region compared to that in the entire STUW domain is likely due to the periodic local ventilation of STUW induced by upwelling, which also leads to an increase in O_2 due to photosynthesis near the surface. STUW O_2 in Region 1 includes the southeastern Caribbean, which undergoes seasonal upwelling [Rueda-Roa and Muller-Karger, 2013].

The loss rate of STUW O_2 at Hydrostation "S" also tracks shifts in the wintertime AMO (Figure 9). O_2 loss rates at BATS, Hydrostation "S", and Region 2, however, are smaller compared to the overall rate of $-0.75 \mu\text{mol kg}^{-1} \text{ yr}^{-1}$ from the entire STUW domain (Table 2.). The lower O_2 loss rates observed at these two time series sites and Region 2 could be the result of an artifact from skewness of the data toward measurements from summer and fall months at these stations (i.e., June through December; see Figure 2e). The lower frequency of detection of STUW between January and April, when ventilation is highest, compared to summer and fall months, when ventilation is minimal, leads to attenuation of the long-term ventilation signal and thus to apparent lower O_2 loss rates at these two sites and Region 2. Smaller O_2 loss trends in Region 2 than in the entire domain of STUW can also be related to changes in ventilation associated with climate shifts. While in the eastern tropical and subtropical North Atlantic the AMO– (NAO+) phase induces an increase in wind velocities and a decrease in SST, the opposite occurs in a portion of the western North Atlantic, such as around the BATS and Hydrostation "S" stations [Cayan, 1992; Enfield *et al.*, 2001; Marshall *et al.*, 2001; Visbeck *et al.*, 2013]. During the AMO– (NAO+) phase, between the early 1980s and the mid-1990s (Figure 8), westerly winds were weaker and SST was warmer than normal at these stations [Bates, 2001; Gruber *et al.*, 2002; Lomas *et al.*, 2010, 2013]. This likely led to stronger water column stratification and reduced ventilation of STUW. After the mid-1990s, westerlies strengthened and SSTs were cooler than normal at BATS and Hydrostation "S". The wintertime AMO (NAO)

shifted to a positive (neutral-negative) phase through at least 2013. This has led to increased primary production and phytoplankton biomass over this period [Lomas *et al.*, 2013]. These conditions should have favored outcropping and ventilation of STUW in this location.

The average STUW O₂ loss rate at BATS and Hydrostation "S" ($0.33 \pm 0.06 \mu\text{mol kg}^{-1} \text{yr}^{-1}$) over the 1980–2013 period is ~50% lower than the rate estimated for the western subtropical North Atlantic (Region 2; Table 2). The lower STUW O₂ loss rate at BATS and Hydrostation "S" is likely a methodological artifact in the calculation of AO₂A at time series stations. Due to the much smaller sample size than WOD13 data sets, time series stations AO₂A values were obtained using mean O₂ values for the entire water column as opposed to mean values calculated within discrete depth intervals (see section 2). AO₂A values calculated with this technique are sensitive to the vertical distribution of the data. For example, if the sample population is predominantly from surface layers, AO₂A values will be skewed by high O₂ values and negative trends will appear artificially small. The opposite will occur if the data set is dominated by lower O₂ values from the deeper layers. Artificially smaller STUW O₂ negative trends are likely to occur at these two sites since STUW is typically found within the upper ~100 m in this region (Figure 1).

6. Conclusions

Since the 1980s, STUW O₂ in the subtropical North Atlantic declined at an average rate of $-0.75 \mu\text{mol kg}^{-1} \text{yr}^{-1}$. Warming at the site of formation of STUW likely resulted in a decline of STUW O₂ of $\sim 3 \mu\text{mol kg}^{-1}$ over this period. The balance of the STUW O₂ loss is driven by increased AOU affected by changes in STUW ventilation, circulation, and transport. Variability in the O₂ levels within STUW follows the wintertime (January–March) AMO and annual NAO index phases. A significant negative correlation between the mean wintertime (January–March) Atlantic Multidecadal Oscillation (AMO) index and mean annual STUW O₂ anomalies (AO₂A; $R_2=0.32$, $p<0.01$) suggests that STUW O₂ concentrations are likely driven by shifts in trade winds intensity and sea surface temperature between 10° and 30°N in the North Atlantic. The neutral-positive (negative) phase of the mean wintertime AMO (annual NAO) leads to weaker trade winds intensity and positive SST anomalies in the formation region of STUW, while negative (positive) wintertime AMO (annual NAO) phases enhance ventilation and formation rates of this water mass.

Declining rates in STUW O₂ were detected at the CARIACO, BATS, and Hydrostation "S" ship-based ocean biogeochemical time series (-0.71 , -0.28 , and $-0.37 \mu\text{mol kg}^{-1} \text{yr}^{-1}$, respectively). No apparent change in STUW O₂ was observed at ESTOC. The absence of a STUW O₂ trend at ESTOC is likely due to this station's proximity to the formation region of STUW and because STUW is only detected intermittently at ESTOC. The rate of STUW O₂ loss at CARIACO was comparable to those measured within the regional southeastern Caribbean Sea ($-0.58 \mu\text{mol kg}^{-1} \text{yr}^{-1}$) and the entire domain of STUW ($-0.75 \mu\text{mol kg}^{-1} \text{yr}^{-1}$). STUW O₂ loss rates measured at BATS and Hydrostation "S", however, were on average 50% lower than that calculated for the subtropical western North Atlantic ($-0.68 \mu\text{mol kg}^{-1} \text{yr}^{-1}$). This could be attributed to a methodological artifact in the calculation of AO₂A using data from time series stations. In order to clearly discern between shifts in oceanic O₂ pools driven by natural climate variability and those from climate forcing induced by human activities, longer oceanographic time series are needed. Changes in STUW ventilation and transport at scales consistent with variability in the AMO and NAO indices lead to significant interannual changes of the STUW O₂ inventory. Sustained neutral-positive AMO conditions could lead to further deoxygenation in tropical and subtropical North Atlantic upper waters.

References

- Astor, Y., F. Muller-Karger, and M. I. Scranton (2003), Seasonal and interannual variation in the hydrography of the Cariaco Basin: Implications for basin ventilation, *Cont. Shelf Res.*, 23(1), 125–144.
- Barnston, A. G., and R. E. Livezey (1987), Classification, seasonality, and persistence of low-frequency atmospheric circulation patterns, *Mon. Weather Rev.*, 115, 1083–1126.
- Bates, N. R. (2001), Interannual variability of oceanic CO₂ and biogeochemical properties in the Western North Atlantic subtropical gyre, *Deep Sea Res., Part I*, 48(8–9), 1507–1528.
- Bopp, L., C. Le Quéré, M. Heimann, A. C. Manning, and P. Monfray (2002), Climate-induced oceanic oxygen fluxes: Implications for the contemporary carbon budget, *Global Biogeochem. Cycles*, 16(2), 1022, doi:10.1029/2001GB001445.
- Bopp, L., *et al.* (2013), Multiple stressors of ocean ecosystems in the 21st century: Projections with CMIP5 models, *Biogeosciences*, 10(10), 6225–6245.
- Casey, K. S., T. B. Brandon, P. Cornillon, and R. Evans (2010), The past, present and future of the AVHRR Pathfinder SST program, in *Oceanography From Space: Revisited*, edited by V. Barale, J. F. R. Gower, and L. Alberotanza, Springer, Netherlands, doi:10.1007/978-90-481-8681-5_16.

Acknowledgments

This work was supported by the National Science Foundation (NSF, grants OCE-0752139, OCE-9216626, OCE-9729284, OCE-9401537, OCE-9729697, OCE-9415790, OCE-9711318, and OCE0963028), the Consejo Nacional de Investigaciones Científicas y Tecnológicas (CONICIT, Venezuela, grant 96280221), the Venezuelan Fondo Nacional de Ciencia y Tecnología (FONACIT, Venezuela, grant 2000001702), and NASA grants NNX14AP62A, NNX11AP76G, and NNX09AV24G. We thank Daniel Otis for providing MATLAB codes for spatial visualization of data and insightful comments on how to process NODC data sets efficiently. We also thank Hernán García from NOAA's NODC/Ocean Climate Laboratory for providing guidance on handling of NODC data records. We are indebted to the personnel of the Fundación La Salle de Ciencias Naturales, Estación de Investigaciones Marinas, Isla Margarita (FLASA/EDIMAR), Estación Europea de Series Temporales Oceánicas de Canarias, and Bermuda Atlantic Time-series Study who have been responsible for the collection, analysis, and quality control of data presented here. Access to all data for this paper is properly described in section 2 and cited and referred to in the reference list.

- Cayan, D. R. (1992), Latent and sensible heat flux anomalies over the northern oceans: The connection to monthly atmospheric circulation, *J. Clim.*, *5*, 354–369.
- Chollett, I., F. E. Müller-Karger, S. F. Heron, W. Skirving, and P. J. Mumby (2012), Seasonal and spatial heterogeneity of recent sea surface temperature trends in the Caribbean Sea and southeast Gulf of Mexico, *Mar. Pollut. Bull.*, *64*(5), 956–965.
- Church, M. J., M. W. Lomas, and F. E. Müller-Karger (2013), Sea change: Charting the course for biogeochemical ocean time-series research in a new millennium, *Deep Sea Res., Part II*, *93*, 2–15.
- Curry, R., B. Dickson, and I. Yashayaev (2003), A change in the freshwater balance of the Atlantic Ocean over the past four decades, *Nature*, *426*, 826–829.
- Deutsch, C., S. Emerson, and L. Thompson (2005), Fingerprints of climate change in North Pacific oxygen, *Geophys. Res. Lett.*, *32*, L16604, doi:10.1029/2005GL023190.
- Doney, S. C., J. L. Bullister, and R. Wanninkhof (1998), Climatic variability in upper ocean ventilation rates diagnosed using chlorofluorocarbons, *Geophys. Res. Lett.*, *25*, 1399–1402, doi:10.1029/98GL00844.
- Ekau, W., H. Auel, H. O. Portner, and D. Gilbert (2010), Impacts of hypoxia on the structure and processes in pelagic communities (zooplankton, macro-invertebrates and fish), *Biogeosciences*, *7*(5), 1669–1699.
- Emerson, S. R., and S. Bushinsky (2014), Oxygen concentrations and biological fluxes in the open ocean, *Oceanography*, *27*(1), 168–171.
- Emerson, S., S. Mecking, and J. Abell (2001), The biological pump in the subtropical North Pacific Ocean: Nutrient sources, Redfield ratios and recent changes, *Global Biogeochem. Cycles*, *15*, 535–554, doi:10.1029/2000GB001320.
- Emerson, S., T. W. Watanabe, T. Ono, and S. Mecking (2004), Temporal trends in apparent oxygen utilization in the upper pycnocline of the North Pacific: 1980–2000, *J. Oceanogr.*, *60*, 139–147.
- Enfield, D. B., and A. M. Mestas-Nunez (1999), Multiscale variabilities in global sea surface temperatures and their relationships with tropospheric climate patterns, *J. Clim.*, *12*(9), 2719–2733.
- Enfield, D. B., A. M. Mestas-Nunez, and P. J. Trimble (2001), The Atlantic Multidecadal Oscillation and its relationship to rainfall and river flows in the continental U.S., *Geophys. Res. Lett.*, *28*, 2077–2080, doi:10.1029/2000GL012745.
- Frölicher, T. L., F. Joos, G. K. Plattner, M. Steinacher, and S. C. Doney (2009), Natural variability and anthropogenic trends in oceanic oxygen in a coupled carbon cycle–climate model ensemble, *Global Biogeochem. Cycles*, *23*, GB1003, doi:10.1029/2008GB003316.
- García, H. E., and L. I. Gordon (1992), Oxygen solubility in seawater: Better fitting equations, *Limnol. Oceanogr.*, *37*(6), 1307–1312, doi:10.4319/lo.1992.37.6.1307.
- García, H., A. Cruzado, L. Gordon, and J. Escanez (1998), Decadal-scale chemical variability in the subtropical North Atlantic deduced from nutrient and oxygen data, *J. Geophys. Res.*, *103*, 2817–2830, doi:10.1029/97JC03037.
- Goldenberg, S. B., C. W. Landsea, A. M. Mestas-Nuñez, and W. M. Gray (2001), The recent increase in Atlantic hurricane activity: Causes and implications, *Science*, *293*, 474–479.
- González Taboada, F., and R. Anadón (2012), Patterns of change in sea surface temperature in the North Atlantic during the last three decades: Beyond mean trends, *Clim. Change*, *115*(2), 419–431.
- Gordon, A. L., and C. F. Giulivi (2008), Sea surface salinity trends over fifty years within the subtropical North Atlantic, *Oceanography*, *21*(1), 20–29.
- Gruber, N. (2009), Fickle trends in the ocean, *Nature*, *458*, 155–156, doi:10.1038/458155a.
- Gruber, N., C. D. Keeling, and N. R. Bates (2002), Interannual variability in the North Atlantic Ocean carbon sink, *Science*, *298*, 2374–2378.
- Gu, D., and S. Philander (1997), Interdecadal climate fluctuations that depend on exchanges between the tropics and extratropics, *Science*, *275*, 805–807.
- Helm, K. P., N. L. Bindoff, and J. A. Church (2011), Observed decreases in oxygen content of the global ocean, *Geophys. Res. Lett.*, *38*, L23602, doi:10.1029/2011GL049513.
- Hurrell, J. W. (1995), Decadal trends in the North Atlantic Oscillation: Regional temperatures and precipitation, *Science*, *269*, 676–679.
- Hurrell, J. W. (1996), Influence of variations in extratropical wintertime teleconnections on Northern Hemisphere temperature, *Geophys. Res. Lett.*, *23*, 665–668, doi:10.1029/96GL00459.
- Jenkins, W. J., and J. Goldman (1985), Seasonal oxygen cycling and primary production in the Sargasso Sea, *J. Mar. Res.*, *43*, 465–491.
- Johnson, D. R., T. P. Boyer, H. E. Garcia, R. A. Locarnini, O. K. Baranova, and M. M. Zweng (2013), World Ocean Database 2013 User's Manual. Sydney Levitus, Ed.; Alexey Mishonov, Technical Ed.; NODC Internal Report 22, NOAA Printing Office, Silver Spring, Md., 172 pp. [Available at <http://www.nodc.noaa.gov/OC5/WOD13/docwod13.html>]
- Johnson, G. C., and N. Gruber (2007), Decadal water mass variations along 20°W in the northeastern Atlantic Ocean, *Prog. Oceanogr.*, *73*(3–4), 277–295.
- Joos, F., G. K. Plattner, T. F. Stocker, A. Körtzinger, and D. W. R. Wallace (2003), Trends in marine dissolved oxygen: Implications for ocean circulation changes and the carbon budget, *Eos Trans. AGU*, *84*(21), 197–201.
- Keeling, R. F., and H. E. Garcia (2002), The change in oceanic O₂ inventory associated with recent global warming, *Proc. Natl. Acad. Sci. U.S.A.*, *99*(12), 7848–7853.
- Keeling, R. F., A. Körtzinger, and N. Gruber (2010), Ocean deoxygenation in a warming world, *Annu. Rev. Mar. Sci.*, *2*, 199–229, doi:10.1146/annurev.marine.
- Kerr, R. A. (2000), A North Atlantic climate pacemaker for the centuries, *Science*, *288*, 1984–1986.
- Locarnini, R. A., A. V. Mishonov, J. I. Antonov, T. P. Boyer, H. E. Garcia, O. K. Baranova, M. M. Zweng, and D. R. Johnson (2010), *World Ocean Atlas 2009, Volume 1: Temperature*, NOAA Atlas NESDIS, vol. 68, edited by S. Levitus, pp. 184, U.S. Gov. Print. Off., Washington, D. C.
- Lomas, M. W., D. K. Steinberg, T. Dickey, C. A. Carlson, N. B. Nelson, R. H. Condon, and N. R. Bates (2010), Increased ocean carbon export in the Sargasso Sea linked to climate variability is countered by its enhanced mesopelagic attenuation, *Biogeosciences*, *7*(1), 57–70.
- Lomas, M. W., N. R. Bates, R. J. Johnson, A. H. Knap, D. K. Steinberg, and C. A. Carlson (2013), Two decades and counting: 24-years of sustained open ocean biogeochemical measurements in the Sargasso Sea, *Deep Sea Res., Part II*, *93*, 16–32.
- Lorenzoni, L. (2012), Sediment transport and distribution over continental shelves: A glimpse at two different river-influenced systems, the Cariaco Basin and the Amazon Shelf, PhD dissertation, Univ. of South Florida.
- Marshall, J., Y. Kushnir, D. Battisti, P. Chang, A. Czaja, R. Dickson, J. Hurrell, M. McCartney, R. Saravanan, and M. Visbeck (2001), North Atlantic climate variability: Phenomena, impacts and mechanisms, *Int. J. Climatol.*, *21*, 1863–1898.
- Meehl, G. A., et al. (2007), Global climate projections, in *Climate Change 2007: The Physical Science Basis: Contribution of Working Group I to the Fourth Assessment Report of the Intergovernmental Panel on Climate Change*, edited by S. Solomon et al., pp. 747–845, Cambridge Univ. Press, New York.
- Müller-Karger, F. E., et al. (2015), Natural variability of surface oceanographic conditions in the offshore Gulf of Mexico, *Prog. Oceanogr.*, doi:10.1016/j.pocean.2014.12.007.
- Müller-Karger, F. E., J. J. Walsh, R. H. Evans, and M. B. Meyers (1991), On the seasonal phytoplankton concentration and sea surface temperature cycles of the Gulf of Mexico as determined by satellites, *J. Geophys. Res.*, *96*, 12,645–12,665, doi:10.1029/91JC00787.

- Muller-Karger, F., et al. (2001), Annual cycle of primary production in the Cariaco Basin: Response to upwelling and implications for vertical export, *J. Geophys. Res.*, 106(C3), 4527–4542, doi:10.1029/1999JC000291.
- Muller-Karger, F., et al. (2013), The CARIACO Ocean Time-Series: 18 years of international collaboration in ocean biogeochemistry and ecological research Ocean Carbon and Biogeochemistry Newsletter, Woods Hole Oceanographic Institution - winter edition.
- O'Connor, B. M., R. A. Fine, and D. B. Olson (2005), A global comparison of subtropical underwater formation rates, *Deep Sea Res., Part I*, 52(9), 1569–1590.
- Pörtner, H.-O., D. M. Karl, P. W. Boyd, W. W. L. Cheung, S. E. Lluch-Cota, Y. Nojiri, D. N. Schmidt, and P. O. Zavialov (2014), Ocean systems, in *Climate Change 2014: Impacts, Adaptation, and Vulnerability. Part A: Global and Sectoral Aspects. Contribution of Working Group II to the Fifth Assessment Report of the Intergovernmental Panel on Climate Change*, edited by C. B. Field et al., pp. 411–484, Cambridge Univ. Press, Cambridge, U. K., and New York.
- Prince, E. D., and C. P. Goodyear (2006), Hypoxia-based habitat compression of tropical pelagic fishes, *Fish. Oceanogr.*, 15(6), 451–464.
- Prince, E. D., J. G. Luo, C. P. Goodyear, J. P. Hoolihan, D. Snodgrass, E. S. Orbesen, J. E. Serafy, M. Ortiz, and M. J. Schirripa (2010), Ocean scale hypoxia-based habitat compression of Atlantic istiophorid billfishes, *Fish. Oceanogr.*, 19(6), 448–462.
- Qu, T., S. Gao, and I. Fukumori (2013), Formation of salinity maximum water and its contribution to the overturning circulation in the North Atlantic as revealed by a global general circulation model, *J. Geophys. Res. Oceans*, 118, 1982–1994, doi:10.1002/jgrc.20152.
- Redfield, A. C. (1934), *On the Proportions of Organic Derivatives in Sea Water and Their Relation to the Composition of Plankton*, James Johnstone Memorial Volume, edited by R. J. Daniel, pp. 177–192, Univ. Press of Liverpool, Liverpool, U. K.
- Rueda-Roa, D. T., and F. E. Muller-Karger (2013), The southern Caribbean upwelling system: Sea surface temperature, wind forcing and chlorophyll concentration patterns, *Deep Sea Res., Part I*, 78, 102–114.
- Schlesinger, M. E., and N. Ramankutty (1994), An oscillation in the global climate system of period 65–70 years, *Nature*, 367, 723–726.
- Schlitzer, R. (2012), Ocean Data View. [Available at <http://odv.awi.de>.]
- Schott, F. A., J. P. McCreary Jr., and G. C. Johnson (2004), Shallow overturning circulations of the tropical-subtropical oceans, in *Earth's Climate: The Ocean-Atmosphere Interaction*, *Geophys. Monogr. Ser.*, vol. 147, edited by C. Wang, S. P. Xie, and J. A. Carton, 261–304, AGU, Washington, D. C., doi:10.1029/147GM15.
- Scranton, M. I., G. T. Taylor, R. Thunell, C. R. Benitez-Nelson, F. Muller-Karger, K. Fanning, L. Lorenzoni, E. Montes, R. Varela, and Y. Astor (2014), Interannual and subdecadal variability in the nutrient geochemistry of the Cariaco Basin, *Oceanography*, 27(1), 148–159.
- Shcherbina, A. Y., E. A. D'Asaro, S. C. Riser, and W. S. Kessler (2015), Variability and interleaving of upper-ocean water masses surrounding the North Atlantic salinity maximum, *Oceanography*, 28(1), 106–113, doi:10.5670/oceanog.2015.12.
- Stendardo, I., and N. Gruber (2012), Oxygen trends over five decades in the North Atlantic, *J. Geophys. Res.*, 117, C11004, doi:10.1029/2012JC007909.
- Stramma, L., G. C. Johnson, J. Sprintall, and V. Mohrholz (2008), Expanding oxygen-minimum zones in the tropical oceans, *Science*, 320, 655–658.
- Stramma, L., S. Schmidtko, L. A. Levin, and G. C. Johnson (2010), Ocean oxygen minima expansions and their biological impacts, *Deep Sea Res., Part I*, 57(4), 587–595.
- Stramma, L., E. D. Prince, S. Schmidtko, J. Luo, J. P. Hoolihan, M. Visbeck, D. W. R. Wallace, P. Brandt, and A. Koertzing (2012), Expansion of oxygen minimum zones may reduce available habitat for tropical pelagic fishes, *Nat. Clim. Change*, 2(1), 33–37.
- Tanhua, T., and R. F. Keeling (2012), Changes in column inventories of carbon and oxygen in the Atlantic Ocean, *Biogeosciences*, 9, 4819–4833, doi:10.5194/bg-9-4819-2012.
- Taylor, G. T., et al. (2012), Ecosystem responses in the southern Caribbean Sea to global climate change, *Proc. Natl. Acad. Sci. U.S.A.*, 109(47), 19,315–19,320, doi:10.1073/pnas.1207514109.
- Vincze, M., and I. M. Janosi (2011), Is the Atlantic Multidecadal Oscillation (AMO) a statistical phantom?, *Nonlinear Process. Geophys.*, 18, 469–475.
- Visbeck, M., H. Cullen, G. Krahnmann, and N. Naik (1998), An ocean model's response to North Atlantic Oscillation-like wind forcing, *Geophys. Res. Lett.*, 25(24), 4521–4524, doi:10.1029/1998GL900162.
- Visbeck, M., E. P. Chassignet, R. G. Curry, T. L. Delworth, R. R. Dickson, and G. Krahnmann (2013), The ocean's response to North Atlantic Oscillation variability, in *The North Atlantic Oscillation: Climatic Significance and Environmental Impact*, edited by J. W. Hurrell, et al., AGU, Washington, D. C., doi:10.1029/134GM06.
- Whitney, F. A., H. J. Freeland, and M. Robert (2007), Persistently declining oxygen levels in the interior waters of the eastern subarctic Pacific, *Prog. Oceanogr.*, 75(2), 179–199.
- Wust, G. (1964), *Stratification and Circulation in the Antillean-Caribbean Basins: Part 1. Spreading and Mixing of the Water Types*, pp. 201, Columbia Univ. Press, New York.

Erratum

In the originally published version of this article, Table 2 contained a typesetting error. This has since been corrected and this version may be considered the authoritative version of record.